Intelligent Hybrid Vehicle Power Control - Part I: Machine Learning of Optimal Vehicle Power

Yi L. Murphey[1], *Senior Member, IEEE*, Jungme Park[1], ZhiHang Chen[1], Ming Kuang[2], *Member, IEEE*, Abul Masrur[3], *Fellow, IEEE*, Anthony Phillips[2]

[1]Department of Electrical and Computer Engineering, University of Michigan-Dearborn
(Phone: 313-593-5028, Fax: 313-583-6336, Email: yilu@umich.edu)
[2]Ford Motor Company, Dearborn, MI, USA.
[3]The US Army RDECOM-TARDEC, Warren, MI 49307.

Abstract— **Energy management in Hybrid Electric Vehicles (HEV) has been actively studied recently because of its potential to significantly improve fuel economy and emission control. Because of the dual-power-source nature and the complex configuration and operation modes in a HEV, energy management is more complicated and important than in a conventional vehicle. Most of the existing vehicle power optimization approaches do not incorporate knowledge about driving patterns into their vehicle energy management strategies. Our approach is to use machine learning technology combined with roadway type and traffic congestion level specific optimization to achieve quasi-optimal energy management in hybrid vehicles. In this series of two papers, we present a machine learning framework that combines Dynamic Programming with machine learning to learn about roadway type and traffic congestion level specific energy optimization, and an integrated online intelligent power controller to achieve quasi-optimal energy management in hybrid vehicles. These two papers cover the modeling of power flow in HEVs, mathematical background of optimization in energy management in HEV, machine learning algorithms and real-time optimal control of energy flow in a HEV.**

This first paper presents our research in machine learning for optimal energy management in HEVs. We will present a machine learning framework, ML_EMO_HEV, developed for the optimization of energy management in a HEV, machine learning algorithms for predicting driving environments and generating optimal power split for a given driving environment. Experiments are conducted based on a simulated Ford Escape Hybrid vehicle model provided by Argonne National Laboratory's PSAT (Powertrain Systems Analysis Toolkit). Based on the experimental results on the test data, we can conclude that the neural networks trained under the ML_EMO_HEV framework are effective in predicting roadway type and traffic congestion levels, in predicting driving trend and in learning optimal engine speed and optimal battery power from Dynamic Programming.

***Index Terms*— Fuel economy, machine learning, energy optimization, HEV power management**

Report Documentation Page

Form Approved
OMB No. 0704-0188

1. REPORT DATE	2. REPORT TYPE	3. DATES COVERED
30 JUN 2012	**Journal Article**	**30-06-2012 to 30-06-2012**

4. TITLE AND SUBTITLE
Intelligent Hybrid Vehicle Power Control - Part I: Machine Learning of Optimal Vehicle Power

5a. CONTRACT NUMBER
5b. GRANT NUMBER
5c. PROGRAM ELEMENT NUMBER

6. AUTHOR(S)
Abul Masrur; Ming Kuang; ZhiHang Chen; Jungme Park; Yi. Murphey

5d. PROJECT NUMBER
5e. TASK NUMBER
5f. WORK UNIT NUMBER

7. PERFORMING ORGANIZATION NAME(S) AND ADDRESS(ES)
University of Michigan,Department of Electrical Engineering,Dearborn,MI,48128

8. PERFORMING ORGANIZATION REPORT NUMBER
; #23018

9. SPONSORING/MONITORING AGENCY NAME(S) AND ADDRESS(ES)
U.S. Army TARDEC, 6501 E.11 Mile Rd, Warren, MI, 48397-5000

10. SPONSOR/MONITOR'S ACRONYM(S)
TARDEC

11. SPONSOR/MONITOR'S REPORT NUMBER(S)
#23018

12. DISTRIBUTION/AVAILABILITY STATEMENT
Approved for public release; distribution unlimited

13. SUPPLEMENTARY NOTES
Paper submitted to IEEE Transactions on Vehicular Technology

14. ABSTRACT

Energy management in Hybrid Electric Vehicles (HEV) has been actively studied recently because of its potential to significantly improve fuel economy and emission control. Because of the dual-power-source nature and the complex configuration and operation modes in a HEV, energy management is more complicated and important than in a conventional vehicle. Most of the existing vehicle power optimization approaches do not incorporate knowledge about driving patterns into their vehicle energy management strategies. Our approach is to use machine learning technology combined with roadway type and traffic congestion level specific optimization to achieve quasi-optimal energy management in hybrid vehicles. In this series of two papers, we present a machine learning framework that combines Dynamic Programming with machine learning to learn about roadway type and traffic congestion level specific energy optimization, and an integrated online intelligent power controller to achieve quasi-optimal energy management in hybrid vehicles. These two papers cover the modeling of power flow in HEVs, mathematical background of optimization in energy management in HEV, machine learning algorithms and real-time optimal control of energy flow in a HEV. This first paper presents our research in machine learning for optimal energy management in HEVs. We will present a machine learning framework, ML_EMO_HEV, developed for the optimization of energy management in a HEV, machine learning algorithms for predicting driving environments and generating optimal power split for a given driving environment. Experiments are conducted based on a simulated Ford Escape Hybrid vehicle model provided by Argonne National Laboratory's PSAT (Powertrain Systems Analysis Toolkit). Based on the experimental results on the test data, we can conclude that the neural networks trained under the ML_EMO_HEV framework are effective in predicting roadway type and traffic congestion levels, in predicting driving trend and in learning optimal engine speed and optimal battery power from Dynamic Programming.

15. SUBJECT TERMS

Fuel economy, machine learning, energy optimization, HEV power management

16. SECURITY CLASSIFICATION OF:			17. LIMITATION OF ABSTRACT	18. NUMBER OF PAGES	19a. NAME OF RESPONSIBLE PERSON
a. REPORT	b. ABSTRACT	c. THIS PAGE			
unclassified	**unclassified**	**unclassified**	**Same as Report (SAR)**	**22**	

I. INTRODUCTION

Development of new vehicles with high fuel efficiency and less emissions has become a new focus of research in the automobile industry due to growing energy and environmental concerns. Hybrid Electric Vehicles (HEVs) have emerged as a promising advanced technology to improve fuel economy while meeting the tightened emissions standards. The improved fuel economy of HEVs is achieved by optimizing the architecture and the various devices and components of the vehicle system, as well as the energy management strategy that is used to efficiently control the energy flow through the vehicle system. In this research we focus on the issue of optimizing vehicle energy management to improve fuel economy.

An HEV combines two or more energy sources, e.g., internal gasoline combustion engine (ICE) and battery, in its propulsion system to move the vehicle. With the use of a secondary power source, an HEV uses a smaller and more efficient engine in its drivetrain. Because of the dual-power-source nature, the design and implementation of an HEV system is a challenging problem. The power control strategy that splits the power between chemical fuel and stored electricity takes an important role in the overall fuel efficiency and amount of emissions. The goal of the power control strategy is to minimize the total fuel consumption and emissions without sacrificing vehicle performance, safety, and reliability. In order to meet these challenges, it is very important to optimize the architecture and the various devices and components of the vehicle system, as well as the energy management strategy that is used to efficiently control the energy flow through the vehicle system.

Current existing real-time power control strategies are largely based on heuristic control rules/fuzzy logic for control algorithm development. Wipke et al. used a strategy that adopts a rule-based structure in the control logic by defining a set of thresholds through an optimization process [1]. Jeon et al. proposed a rule-based multi-mode driving control strategy for parallel HEVs that uses an algorithm that is optimized for a recognized driving pattern [2]. Zhu et al. implemented a fuzzy rule-based power controller, in that the fuzzy rules are extracted by studying the optimization result for the given cycle [3]-[4]. Schouten et al. implemented a load-leveling and charge-sustaining strategy by using a fuzzy logic technique [5]. These heuristic rules/fuzzy logic-based strategies mostly stem from engineering intuition, which is sometimes far from the actual optimal solution.

An alternative approach is to apply an optimal control method such as linear programming [6], optimal control [7], and especially dynamic programming (DP) [8]-[10] to the power distribution and management problem. In general, these techniques require the knowledge of the entire drive cycle in advance. Therefore they do not offer an online solution. Furthermore, an optimal power split solution for a given specific drive cycle might be neither optimal nor charge-sustaining under other cycles. To address these issues, a number of techniques have been proposed. Paganelli et al. used an instantaneous optimization method that reduces the problem to a minimization of equivalent fuel consumption at each time instance [11]. If only the present state of the vehicle is considered, the optimization of the operating points of the individual components can still be beneficial, however the

benefits will be limited [11]-[13]. Lin et al proposed a stochastic dynamic programming (SDP) method in an attempt to obtain the optimization for general driving conditions, rather than a specific driving cycle, using power demand probability [14].

Recent research has shown that the current driving environment and the driver's driving style have a strong influence over a vehicle's fuel consumption and emissions [15]-[19]. Driving patterns exhibited by a real world driver are the product of the instantaneous decisions of the driver to respond to the (physical) driving environment. Specifically, varying roadway type and traffic congestion level, driving trends, driving styles, and vehicle operating modes have various degrees of impact on fuel consumption. However most of the existing vehicle power optimization approaches do not incorporate knowledge about driving patterns into their vehicle energy management strategies. Our approach is to use machine learning technology combined with roadway type and traffic congestion level specific optimization to achieve quasi-optimal energy management in hybrid vehicles. It is our contribution to use the current driving environment to predict the future driving conditions, train an online energy management system using machine learning to emulate the optimal solutions generated by Dynamic Programming (DP) for specific roadway types and traffic congestion levels, and generalize the optimal power settings to real world vehicle operation based on the predicted real-time roadway types and traffic congestion levels.

This paper, the first in a series of two, presents our research in the development of a machine learning framework, ML_EMO_HEV, for the optimization of energy management in an HEV. In the ML_EMO_HEV framework, algorithms are developed to learn energy optimization based on long and short term knowledge about the driving environment. The long term knowledge about the driving environment is represented by the type of the drive cycle the driver is in for the next few minutes. The short term knowledge is the driver's immediate reaction to the driving environment at each time instance. In the second paper of the series, we will present the intelligent online energy controller developed under the framework of ML_EMO_HEV and trained by the machine learning algorithms presented in this paper to minimize the fuel consumption while maintaining vehicle performance.

The paper is organized as follows. Section II introduces an HEV model and energy optimization in an HEV. Section III presents the machine learning technologies we developed for optimal vehicle energy management. Section IV concludes this paper.

II. ENERGY OPTIMIZATION IN AN HEV

The energy management problem for HEVs is a dynamic optimization problem. In the discrete time format, the dynamics of an HEV system can be defined by the state transition equation:

$$x(t+1) = f(x(t), u(t), t) \tag{1}$$

where $u(t)$ is the vector of control variables such as engine speed, engine power and battery charging or discharging power, and $x(t)$ is the state variable in the HEV system, which is represented by the battery state of charge level. The HEV system can be interpreted as taking the action of control variables at time *t*, $u(t)$ at the given state $x(t)$ and transforming the vehicle to the next state $x(t+\Delta t),\ \Delta t > 0$. The energy optimization of the HEV can be formulated as follows:

$$\min_{\bar{u}} F(\bar{x},\bar{u}) \text{ subject to } C(\bar{x},\bar{u}) \le 0 \tag{2}$$

where $F(\bar{x},\bar{u})$ is the objective function (or cost function), $C(\bar{x},\bar{u})$ is the constraints on variables. Because our goal of vehicle energy management is to minimize the total fuel cost over a given drive cycle, the objective function $F(\bar{x},\bar{u})$ represents the accumulated fuel cost:

$$F(\bar{x},\bar{u}) = \sum_{t=1}^{N} fuel\_rate(x(t),u(t),t)\Delta t \tag{3}$$

where *N* is the horizon or number of times that the control is applied, $\bar{x} = < x(1),..., x(N) >$ and $\bar{u} = < u(1),..., u(N) >$. The energy optimization problem is solved using Dynamic Programming (DP) based on the dynamics of the power split HEV.

II.1 Power flow in an HEV vehicle

Figure 1 shows power flow in a power split HEV configuration, in which conventional definitions of signs for motor, generator, and battery power are represented by the arrows. P_{gen}, P_{gen_e}, P_{mot}, P_{mot_e}, P_{batt} and P_s can flow in both directions, where P_{gen} is the (mechanical) generator power, P_{gen_e} is the electrical generator power, P_{mot} is the (mechanical) motor power, P_{mot_e} is the electrical motor power, P_{batt} is the power output of the battery and P_s is the internal battery power. A power flows in the direction of an arrow is positive, otherwise it is negative. When the power of an electric machine flows in the positive direction, it indicates that the electric machine is motoring; otherwise, is generating.

The output power from the engine, P_{eng} can be split into the power at ring gear, P_{ring} and the power at generator, P_{gen}. The ring gear power, P_{ring}, represents the mechanical power flow path from the engine to the ring gear to the final drive. The generator power, P_{gen}, represents an electrical path from the engine to the generator to the motor to the final drive. The split of the engine output power between the mechanical path and the electrical path is accomplished by controlling the engine speed with the generator. The electrical motor draws the power from the battery and propels the vehicle. The two power paths provide propulsion power to the final drive to move the vehicle forward simultaneously or independently [21].

The battery used in this research is a Nickel Metal Hydride (NiMH) battery. As shown in Figure 1, the battery model is represented by a battery efficiency component and an energy storage component. The battery power is defined as positive when it

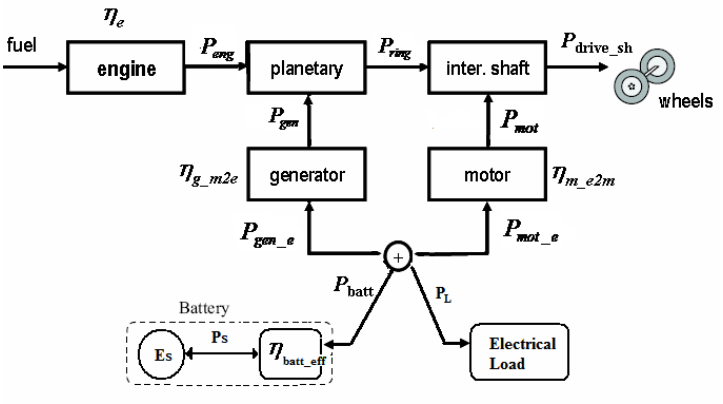

Figure 1. Power flow in a Split HEV configuration with arrows indicating positive power.

is charging and as negative when it is discharging. The battery efficiency component determines the energy loss during the charging and discharging in the battery. The internal battery power, P_s is defined as $P_s(t) = V_{oc}(T,SOC) * I(t)$, where V_{oc} is the open circuit voltage in the battery model, T is the battery temperature, and I is the battery current. The current, I is calculated by $I = \frac{1}{2 \times R_{resist}} \left\{ -V_{oc} + \sqrt{V_{oc}^2 + 4 \times R_{resist} \times P_{batt}} \right\}$, where R_{resist} is the battery internal resistance. Based on the equation above, the open circuit voltage V_{oc} varies depending on SOC and the temperature. But in reality, V_{oc} in NiMH batteries varies only a little within the SOC range 20~80% [22].

The energy storage block keeps track of the energy level in the battery. The charge level of the battery, Q is represented by the integration of the current, I

$$Q(t) = Q(0) + \sum_{k=0}^{t} I(k)\Delta k \,. \tag{4}$$

Because the proposed battery model is power based and available SOC range is 40~60%, the battery energy level, $E(t)$ [J] is used as a state variable in the energy control problem. The battery energy level, $E(t)$ is defined as below

$$E(t) = E(0) + \sum_{k=0}^{t} P_s(k)\Delta k \cdot \tag{5}$$

The power split HEV system allows two degrees of freedom in energy optimization, which we can represented by two control variables, the engine speed, ω_{eng} and the battery power, P_{batt}. The control variables at time t are defined as $u(t) = (P_{batt}(t), \omega_{eng}(t))$. Once the values of two control variables are obtained, then the speed and power of the other components (the engine, the motor, and the generator) can be determined based on the kinematics and dynamics of the power split HEV system. The optimization is subject to the individual components constraints in the system: engine, generator, motor and battery. The operating range of each component is limited in the energy optimization. The inequality constraints for each component are introduced to the limit minimum and maximum power flow defined as follows:

$$
\begin{aligned}
&0 \le P_{eng}(t) \le P_{eng\_\max}(\mathrm{t}), \quad 0 \le \omega_{\mathrm{eng}}(t) \le \omega_{eng\_\max}(t) && \forall t \in [1, N] \\
&P_{gen\_\min}(t) \le P_{gen}(t) \le P_{gen\_\max}(t), \quad \omega_{gen\_\min}(t) \le \omega_{\mathrm{gen}}(t) \le \omega_{\mathrm{gen\_max}}(t) && \forall t \in [1, N] \\
&P_{mot\_\min}(t) \le P_{mot}(t) \le P_{mot\_\max}(t), \quad \omega_{mot\_\min}(t) \le \omega_{\mathrm{mot}}(t) \le \omega_{\mathrm{mot\_max}}(t) && \forall t \in [1, N] \\
&P_{batt\_\min}(t) \le P_{batt}(t) \le P_{batt\_\max}(t) && \forall t \in [1, N]
\end{aligned} \tag{6}
$$

where P_{*_min} is the minimum power of the corresponding component, and P_{*_max} is the maximum power of the corresponding component. Similarly, ω_{*_min} is the minimum speed of the corresponding component, and ω_{*_max} is the maximum speed of the corresponding component.

In order to create a well-posed problem, an end point constraint is imposed on the state variable, *E*, requiring the energy level at the end of the given drive cycle to be the same as the initial energy level

$$E(N) = E(0) => \sum_{k=1}^{N} P_s(k)\Delta k = 0. \tag{7}$$

By combining these inequality constraints and the end point constraint with the objective function we can ensure that the engine speed, the battery energy level, engine power, generator power and motor power are all within their corresponding boundaries in the optimal solution.

In the HEV energy management problem, the objective of DP is to find the optimal sequence of control variables, $\bar{u} = < u(1), ..., u(N) >$, that minimizes the accumulated fuel cost over a given drive cycle. Since the objective is to minimize fuel cost, the calculation of the instantaneous fuel consumption based on the given control variables is critical. To this end, a nonlinear static engine efficiency map provided by the manufacturer is used to describe the relationship between fuel consumption and the state and control variables. Specifically, the instantaneous fuel cost is a function of engine speed and engine power, denoted as $\Phi_{eng}(P_{eng}, \omega_{eng})$. Assuming the moment of inertia of the engine is negligible and the vehicle speed, v_s, vehicle electrical load, P_L, and the driver's power demand, P_{drive_sh} are known, the instantaneous engine power P_{eng} for the given control variable $u(t) = (P_{batt}(t), \omega_{eng}(t))$ can be calculated based on the kinematic equations of the HEV as follows:

Step 1: Calculate the motor speed, ω_{mot} given the current vehicle speed v_s

$$\omega_{mot} = \omega_{ring} = \frac{v_s}{wheel\_r} \times fd\_ratio \tag{8}$$

where *wheel_r* is the effective wheel radius and *fd_ratio* is the final drive ratio.

Step 2: Calculate the generator speed, ω_{gen} and the sun gear speed, $\omega_{sun,}$

$$\omega_{gen} = \omega_{sun} = \omega_{eng} \frac{N_{ring} + N_{sun}}{N_{sun}} - \omega_{mot} \frac{N_{ring}}{N_{sun}} \tag{9}$$

where N_{sun} is number of teeth of the sun gear and N_{ring} is number of teeth of the ring gear.

Step 3: Calculate motor power loss, P_{mot_loss} and generator power loss, P_{gen_loss}. These power losses depend on the motor and the generator efficiencies given motor and generator torque and speed.

Step 3.1: Calculate the desired engine power, P_{eng}^{*} at steady system operation using the given battery power P_{batt}, the driver's power demand, P_{drive_sh} and the electrical load as:

$$P_{eng}^{*} = P_{drive\_sh} + P_{batt} + P_{L}. \tag{10}$$

This desired engine power, P_{eng}^{*} is the engine power at the steady system and it is used to calculate the generate torque τ_{gen} and motor torque τ_{mot} at the next step.

Step 3.2: Calculate the generator torque τ_{gen} and motor torque τ_{mot}. The desired engine torque, τ_{eng}^{*} is first calculated by $\tau_{eng}^{*} = P_{eng}^{*} / \omega_{eng}$. Then the estimated generator torque, τ_{gen}, and ring gear torque, τ_{ring}, are calculated as follows:

$$\tau_{gen} = \frac{N_{sun}}{N_{ring}+N_{sun}} \tau_{eng}^{*}, \quad \tau_{ring} = \frac{N_{ring}}{N_{ring}+N_{sun}} \tau_{eng}^{*}. \tag{11}$$

The motor torque, τ_{mot} is calculated based on the fact that the driver's power demand, $P_{drive\_sh,}$ in the power split HEV is equal to the power at ring gear, P_{ring} plus the motor power, P_{mot}, i.e.

$$P_{drive\_sh} = P_{ring} + P_{mot} = \tau_{ring}\omega_{ring} + \tau_{mot}\omega_{mot} = (\tau_{ring}+\tau_{mot})\omega_{mot}.$$

$$\tau_{mot} = (P_{drive\_sh} / \omega_{mot}) - \tau_{ring} \tag{12}$$

Step 3.3: Using efficiency maps of the generator and the motor, calculate generator power loss, P_{gen_loss} and motor power loss, P_{mot_loss} as follows:

$$P_{gen\_loss} = \eta_{gen}(\omega_{gen}, \tau_{gen}), \quad P_{mot\_loss} = \eta_{mot}(\omega_{mot}, \tau_{mot}) \tag{13}$$

where η_{gen} is a generator efficiency map and η_{mot} is a motor efficiency map.

Step 4: Calculate the final engine power, P_{eng}:

$$P_{eng} = P_{drive\_sh} + P_{batt} + P_{mot\_loss} + P_{gen\_loss} + P_{L}. \tag{14}$$

With two control variables, battery power, P_{batt} and engine speed, ω_{eng} the corresponding engine power is calculated using equations (8)-(14). Then the instantaneous fuel rate can be expressed as a function of the control variables $u(t) = (P_{batt}(t), \omega_{eng}(t))$ as below:

$$\Phi_{eng}(P_{eng}(t), \omega_{eng}(t)) = fuel\_rate(P_{batt}(t), \omega_{eng}(t) \mid P_{drive\_sh}(t), P_{L}(t)). \tag{15}$$

The objective function, $F(\bar{x}, \bar{u})$ for the power split HEV optimization is then expressed in equation (16).

$$F(\bar{x}, \bar{u}) = \sum_{t=1}^{N} fuel\_rate(P_{batt}(t), \omega_{eng}(t) \mid P_{drive\_sh}(t), P_{L}) \tag{16}$$

II.2. Energy Optimization in an HEV using Dynamic Programming

The energy optimization problem in an HEV for a given drive cycle, *V(t),* can be considered as a problem of optimization of a sequence of dynamic states. Dynamic Programming (DP) is used to find the optimal control variables at every time step of the drive cycle as shown in equation (17).

$$\min_{\bar{u}} F(\bar{x},\bar{u}) = \min_{P_{batt},\omega_{eng}} \sum_{t=1}^{N} fuel\_rate(P_{batt}(t),\omega_{eng}(t) \mid P_{drive\_sh}(t),P_L) \tag{17}$$

where the driver's power demand, $P_{drive\_sh}(t)$ is a function of *V(t).* The sampling time, Δt for the HEV control problem is selected to be 1 second because the SOC changes slowly and 1 second sampling time is sufficient. The DP optimization algorithm is a multi-step decision process. Based on the principal of optimality, DP finds the sequence of optimal battery power, $P_{batt}(t)$, and engine speed, $\omega_{eng}(t)$, values that minimize the total fuel consumption over the entire drive cycle *V(t)* while satisfying all constraints. In implementation, we build a cost to go matrix, *R*, (see Figure 2) based on the battery energy level, *E*, and engine speed, ω_{eng}, in the temporal domain. The two control variables, P_{batt} and ω_{eng}, and the state variable, *E*, are quantized into grids. In Figure 2, the engine speed is discretized into 31 different engine speeds and is labeled as an engine index *i*, *i*=1,…, 31. Here engine index 1 = 0 radius/sec and engine index 31 equals the maximum engine speed.

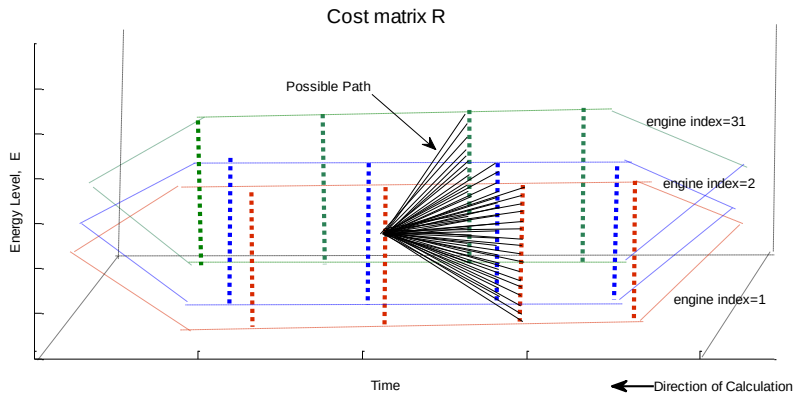

Figure 2. Projection of cost matrix R along the driving cycle.

The cost matrix, *R*, with state entries (*E*, ω_{eng}) keeps track of the minimum fuel cost from the current time, *t*, to the end of the given drive cycle for each combination of states. Then, according to Bellman's principle of optimality, the optimal decision at the t^{th} step is made based on the formula below:

$$\begin{aligned} &R(t,E(t),\omega_{eng}(t)) = 0, \ \text{ if } t = N, \\ &R(t,E(t),\omega_{eng}(t)) \\ &= \min_{P_{batt},\omega_{eng}} [R(t+1,E(t+1),\omega_{eng}(t+1)) + fuel\_rate(P_{batt}(t),\omega_{eng}(t) \mid P_{drive_{sh}}(t),P_L(t))], \ t = (N-1,\cdots,1] \end{aligned} \tag{18}$$

subject to

$$P_{batt\_\min}(t) \le P_{batt}(t) \le P_{batt\_\max}(t),\ \omega_{eng\_\min}(t) \le \omega_{eng}(t) \le \omega_{eng\_\max}(t),\ (t,E(t),\omega_{eng}(t)) \in R,\ (t+1,E(t+1),\omega_{eng}(t+1)) \in R.$$

The recursive equation is solved backwards from $t = N$ to 1 to get the optimal solution. The sequences of optimal battery power, P_{batt}, and optimal engine speed, ω_{eng}, that minimizes the total fuel consumption are given afterwards by starting at $E(1)$ and following the path of minimal cost stored in R.

The minimization of the overall fuel consumption through the appropriate split of mechanical power from the engine and electrical power from the battery is the most critical part in HEV energy management. Varying the power split ratio between the mechanical and electrical paths throughout the drive cycle can result in significantly different fuel economy. The HEV model under our study is a power split power train system, which is used in both Ford Escape hybrid and Toyota Prius. The power train of power split HEV consists of an engine, generator, motor, battery and planetary gear set [20-21].

In the power split HEV system, two power sources are connected to the wheels through a planetary gear set. One power source is the engine, and another is the battery. The combination of an engine and a generator can provide power to the driveline either through an electrical path, a mechanical path or through a combination of the two. The combination of battery, motor, and generator provides power to the driveline using the battery power. Depending on the operation mode, either the engine or the motor or both can provide the traction power to the drivetrain. During vehicle deceleration, the regenerative braking power is captured to charge the battery. In the power split HEV powertrain, the planetary gear set is the key device that connects the engine, generator, and motor to form a power split device. Due to the kinematic property of the planetary gear set, the engine speed can be decoupled from the vehicle speed [21]. This flexibility in the power split HEV system is one of degrees of freedom that can be exploited in the optimization. The focus of this research is the development of machine learning technology to optimize energy consumption over a drive cycle with two control variables, battery power and engine speed, or engine power and engine speed. The proposed machine learning algorithms require the use of a high fidelity vehicle system modeling and simulation program, such as PSAT (Powertrain Systems Analysis Toolkit**),** to build an authentic vehicle model, V, of particular interest.

III. MACHINE LEARNING OF OPTIMAL POWER CONTROL IN AN HEV

The DP optimization of the power split system described in section II assumes that the entire drive cycle $V(t)$, $t = 1, \ldots, N$, is known a priori. However, since knowledge of the future driving speed is not known during real world driving, we cannot directly apply the DP optimization approach in an online energy management solution. Instead, our approach is to predict the driving condition in the near future that can affect the vehicle energy management and use this information to calculate and apply the optimal energy management solution. We developed a machine learning strategy to learn the optimal power split settings for a set of standard drive cycles and then generalized the knowledge to online energy management through neural learning. Figure 3

illustrates the proposed machine learning framework, ML_EMO_HEV. It contains two major machine learning processes: machine learning for driving environment prediction and machine learning for optimal energy management. Specifically, the framework first uses a neural network to model the road environment of a driving trip as a sequence of different roadway types and traffic congestion levels such as local, freeway, arterial/collector, etc., augmented with different traffic congestion levels. This part of the framework uses an additional neural network to model the driver's instantaneous reaction to the driving environment. Then, based on the current predicted roadway type and traffic congestion level and driving trend, the framework uses an additional set of neural networks to emulate the optimal energy management strategy as dictated by DP for the current conditions, in a way that can be implemented in an online environment.

III.1 Machine learning of the driving environment

A. Neural learning for prediction of roadway types and traffic congestion levels

To represent real world driving conditions, Sierra Research, Inc. has developed a set of 11 standard drive cycles presented in [23]-[24], called facility-specific (FS) cycles. These cycles represent passenger car and light truck operations over a broad range of facilities and congestion levels in urban areas. In this research we use this set of 11 FS cycles as the standard measure of roadway types and traffic congestion levels. For the convenience of description we label these 11 FS cycles as $R_1,\ldots, R_{11}$.

Figure 3. ML-EMO-HEV: a computational framework for machine learning of optimal energy management in HEV.

TABLE I
STATISTICS OF 11 FACILITY SPECIFIC DRIVE CYCLES

Drive Cycle	V_{avg} (m/s)	V_{max} (m/s)	A_{max} (m/s^2)	Length (sec)
Freeway LOS A: R_1	30.29	35.54	1.02	399
Freeway LOS B: R_2	29.94	35.01	1.30	366
Freeway LOS C: R_3	29.74	35.19	1.52	448
Freeway LOS D: R_4	29.16	34.66	1.30	433
Freeway LOS E: R_5	25.56	33.26	1.79	471
Freeway LOS F: R_6	14.58	28.53	1.79	536
Freeway Ramps: R_7	15.46	26.90	2.55	266
Arterials LOS A-B: R_8	11.08	26.32	2.23	737
Arterials LOS C-D: R_9	8.58	22.12	2.55	629
Arterials LOS E-F: R_{10}	5.18	17.83	2.59	504
Local : R_{11}	5.77	17.11	1.65	525

Table I shows the most recent definition of these roadway types and traffic congestion level [24] along with the labels we assigned, where V_{avg} is the average vehicle speed, V_{max} is the maximum vehicle speed, and A_{max} is the maximum acceleration. The 11 drive cycles are divided into four categories of roadway types and traffic congestion levels, freeway, freeway ramp, arterial, and local. Two of the categories, freeway and arterial, are further divided into subcategories based on a qualitative measure called level of service (LOS) that describes operational conditions within a traffic stream based on speed and travel time, freedom to maneuver, traffic interruptions, comfort, and convenience. Six types of LOS are defined with labels, *A* through *F*, with LOS A representing the best operating conditions and LOS F the worst. Each level of service represents a range of operating conditions and the driver's perception of those conditions [24]-[25].

With the above definition of standard drive cycles, the problem of optimal vehicle energy management is formulated as follows. Assume that at any time t for a given drive cycle *DC(t)*, ($t \in [0, t_e]$, where t_e is the ending time of the drive cycle), the vehicle is operating according to one of the 11 roadway types and traffic congestion levels, $\boldsymbol{R_i}$, $i = 1, \ldots, 11$. These roadway types and traffic congestion levels will form the basis for calculating the optimal energy management strategy using DP and will also be used as the basis for the online neural network implementation of the DP emulation.

We formulate the problem of roadway type and traffic congestion level prediction as follows. Let $RT[t]$ be the roadway types and traffic congestion levels the driver needs to go through to complete his trip, with $t = 0, 1, \ldots, t_c, \ldots, t_e$ where t_c is the current time instance, and t_e is the time when the trip ends. At any given time t_c, $RT(t_c) \in \{ R_i \mid i = 1, \ldots, 11\}$. We will predict the roadway type and traffic congestion level in the near future based on the short term history of the driver during the trip.

In order to predict the roadway type and traffic congestion level at time t_c, we use the driving speed in the segment $[t_c - \Delta W_{RT}, t_c]$. Here the positive value ΔW_{RT} is the window size of the segment used for making the roadway type and traffic congestion level prediction. The prediction is made at time steps, $k\Delta t_{\mathrm{rt}}$, $k = 1, 2, \ldots$ and is used for calculating the optimal energy management strategy over the time period $[t_c, t_c + \Delta t_{rt}]$. The time interval over which the prediction is made is Δt_{rt}. Figure 4

illustrates these two parameters on the speed profile of the UDDS drive cycle. The x-axis represents the time during the drive cycle and y-axis represents the vehicle speed in miles per hour. For purpose of illustration, the segments shown in Figure 4 have an equal size of ΔW_{RT} = 150 seconds and a time step of Δt_{rt} = 100 seconds. Please note that ΔW_{RT} = 150, Δt_{rt} = 100 seconds are chosen here only for the clarity of the illustration. In reality, as we will show, Δt_{rt} should be much smaller than 100 seconds.

The two parameters are important for the accuracy of the prediction and real-time implementation. Since features characterizing road types and traffic congestion levels are extracted from the speed profile of the vehicle in the time interval [t_c - ΔW_{RT}, t_c], if ΔW_{RT} is too small, the segment may not contain sufficient information. If ΔW_{RT} is too big, the segment may contain obsolete information. Based on our extensive study on these two parameters [26], ΔW_{RT} =50 seconds and Δt_{rt}=1 second are chosen. Our study clearly showed that systems uses Δt_{rt}=1 give significantly better performances over the larger time intervals. ΔW_{RT} = 50 is chosen because it gives shorter delay at the beginning of the drive cycle and is computationally more efficient, which is important for online control. Once ΔW_{RT} is determined, the 14 features presented in TABLE II are extracted from the speed profile within the time. We conducted extensive study on the effectiveness of the window size, various drive cycles, we determined that ΔW_{RT} =50 seconds and Δt_{rt}=1 second are an appropriate window size and prediction time interval, respectively.

We developed a multi-layered and multi-class neural network, NN_RT&TC, for the prediction of roadway types and traffic congestion levels as shown in Figure 5. The performance of the neural network on the 5-fold cross validation is 95% on the training data and 94% on the test data. Detailed training and testing data selection, feature selection algorithms and training process are presented in [26]. When NN_RT&TC is used inside a vehicle to predict the roadway type and traffic congestion level at time t_c, the vector of the 14 features is extracted from the vehicle speed during the time interval, [t_c-50 seconds, t_c].

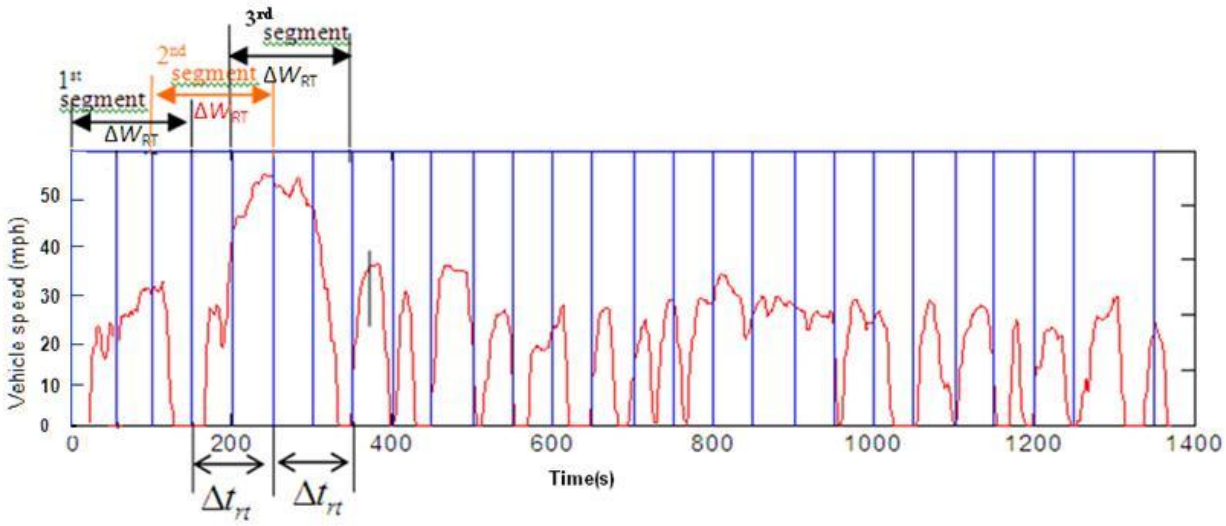

Figure 4. Illustration of segments of a speed profile. The X axis represents time measured in seconds, and the Y axis represents speed measured in mph.

TABLE II
FOURTEEN FEATURES SELECTED FOR ROADWAY TYPE AND TRAFFIC CONGESTION LEVEL PREDICTION

Name of selected features:	Description
Trip distance;	ΔS is distance traveled between t- ΔW_{RT} and t
Maximum speed;	max(v_s(t)), where v_s(t) is speed and $t \in [t-\Delta W_{RT}, t)$
Maximum acceleration;	$\max(a_t^+)$, where a_t^+ is acceleration and $t \in [t-\Delta W_{RT}, t)$
Maximum deceleration	$\max(\mid a_t^- \mid)$, where a_t^- is deceleration and $t \in [t-\Delta W_{RT}, t)$
Average speed	ave(v_s(t)): average of v_s(t), and $t \in [t-\Delta W_{RT}, t)$
Average acceleration	ave(a_t^+): average of a_t^+ and $t \in [t-\Delta W_{RT}, t)$
S. D. of acceleration	$\sqrt{\text{var}(a_t^+)}$ and $t \in [t-\Delta W_{RT}, t)$
Average deceleration	ave(a_t^-) and $t \in [t-\Delta W_{RT}, t)$
% of time in speed interval 0-15 km/h	$P(v_s(t) \mid 0 \le v_s(t) < 15)$ for all $t \in [t-\Delta W_{RT}, t)$
% of time in speed interval 15-30 km/h	$P_{(v_s(t) \mid 15 \le v_s(t) < 30)}$ for all $t \in [t-\Delta W_{RT}, t)$
% of time in speed interval >110 km/h	$P(v_s(t) \mid v_s(t) > 110)$ for all $t \in [t-\Delta W_{RT}, t)$
% of time in deceleration interval (-10)-(-2.5) m/s2	$P\ (a_t^- \mid -10 \le a_t^- < -2.5)$ for all $t \in [t-\Delta W_{RT}, t)$
% of time in deceleration interval (-2.5)-(-1.5) m/s2	$P\ (a_t^- \mid -2.5 \le a_t^- < -1.5)$ for all $t \in [t-\Delta W_{RT}, t)$
Number of acceleration shifts where the acceleration is 0.5~1 m/s2	Number $(a_t^+ \mid 0.5 \le a_t^+ < 1.0)$ for all $t \in [t-\Delta W_{RT}, t)$

The output from NN_RT&TC is the roadway type and traffic congestion level to be used by an intelligent vehicle energy management algorithm to determine the optimal power distribution during time interval [t_c, t_c+1seconds]. Figure 6 shows an example of a drive cycle, LA92, labeled with the actual roadway types and traffic congestion levels for the cycle according to the definition of the 11 standard FS roadway types and traffic congestion levels as defined in [24]. The X axis indicates the time and the Y axis indicates the vehicle speed in miles per hour. The prediction results generated by the neural network NN_RT&TC are shown in the blue color. Notice there is a delay in the prediction for the first 50 seconds due to the need for the algorithm to have at least one window of data available for use in the prediction.

The prediction results of NN_RT&TC for LA92 along with 9 other cycles from PSAT are shown in TABLE III. The percentages given are the prediction accuracy of the neural network calculated as follows: $NN_p = (N_c / N) * 100^{\%}$, where N_c is the number of times during the drive cycle that the neural network makes a correct prediction of the FS roadway type and traffic congestion level, and N is the number of predictions made by the neural network through the entire cycle. The prediction accuracy is high: more than 90% of time, the roadway type and traffic congestion levels are predicted correctly on all drive cycles. On six drive cycles, the prediction accuracy reached more than 95%. The errors are caused by the time delay of the prediction, which is based on the features extracted from a window of past vehicle speed.

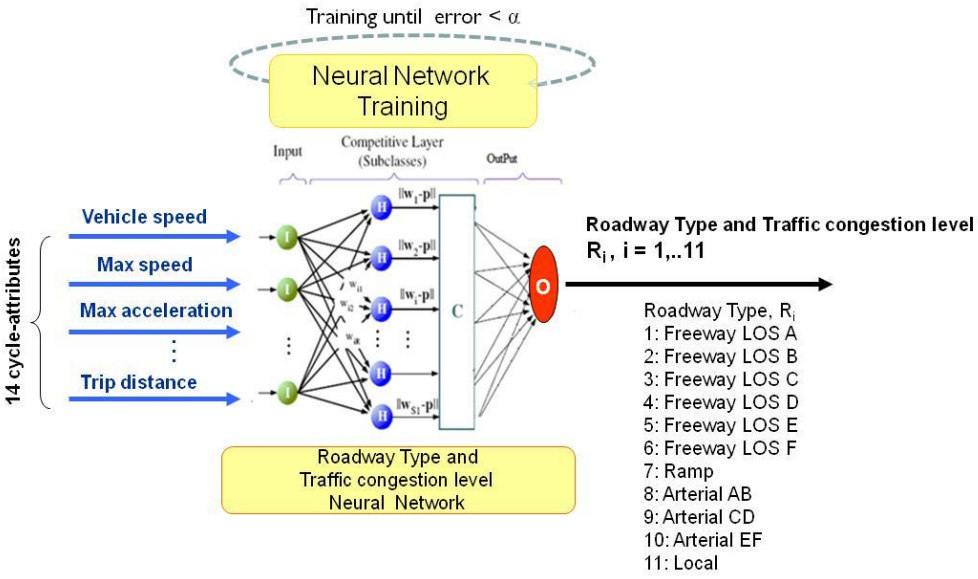

Figure 5. Neural learning for roadway types and traffic congestion levels prediction.

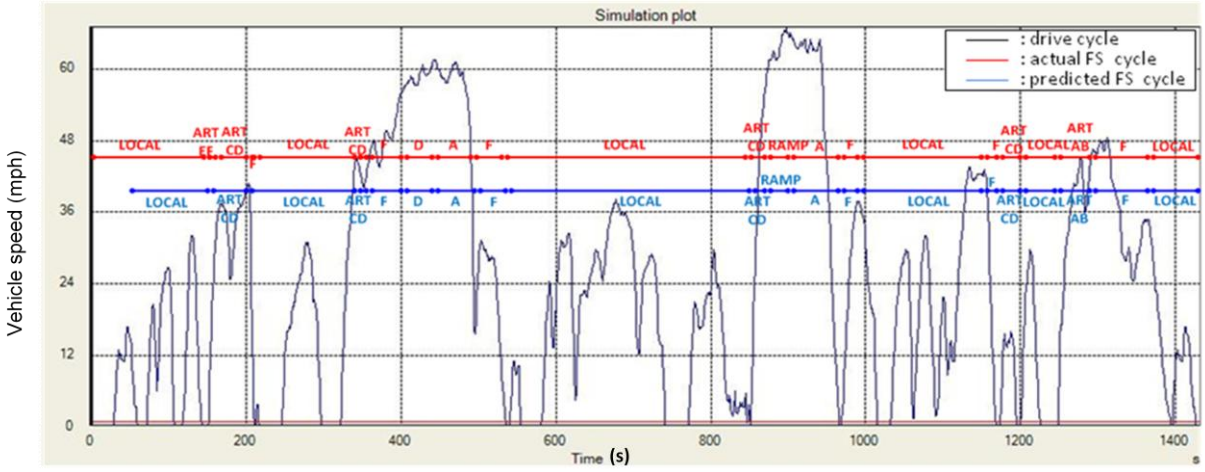

Figure 6. Neural Network performance of roadway types and traffic congestion levels prediction for LA92.

TABLE III
THE PREDICTION PERFORMANCES OF THE NEURAL NETWORK OVER TEST DRIVE CYCLES

Drive cycles	Neural network prediction performance: NN_p (%)		Drive cycles	Neural network prediction performance NN_p (%)
UDDS	97.04		REP05	95.85
HWFET	95.38		NY_CITY	98.72
US06	95.09		HL07	95.96
SC03	90.99		Unif01	94.65
LA92	91.77		Arb02	91.63

B. Neural learning for predicting driving trends

The neural network NN_DT (see Figure 7), is developed for predicting the driving trend at any given time instance *t*. The driving trend is a short term action taken by the driver in the next few seconds. The NN_DT is trained on the following six features from the current vehicle state during the time window $[t-\Delta W_{DT}, t)$: v_{ave}, v_{max}, v_{min}, *ac*, v_{st} *and* v_{end}, where the first four parameters are, respectively, the average speed**,** maximum speed, minimum speed and average acceleration, during the time period $[t-\Delta W_{DT}, t)$, v_{st} is the vehicle speed at $(t-\Delta W_{DT})$, and v_{end} is the vehicle speed at *t*. We define vehicle driving trends into five classes shown in TABLE IV. The quantitative descriptions are used to automatically label the segments in training driving cycles, which are the 11 Sierra Research facility-specific driving cycles. The NN_DT algorithm is a multi-class neural network with 6 input nodes, one hidden layer and 5 output nodes to represent the five classes of driving trends at time interval Δt_{DT} =1(one-step prediction). In order to decide on the optimal size of ΔW_{DT}, we experimented with various sizes on training and test driving cycles and the results are shown in Figure 8. The cycles used for testing the driving trend prediction were the 10 cycles provided by the PSAT simulation system. Based on the performances on both training and test data, ΔW_{DT} =9 seconds is selected as a good window size to use because it gave better performances compare to the performance of smaller window sizes and similar performances to the performance of larger window sizes such as ΔW_{DT} =15, 30, 50 seconds.

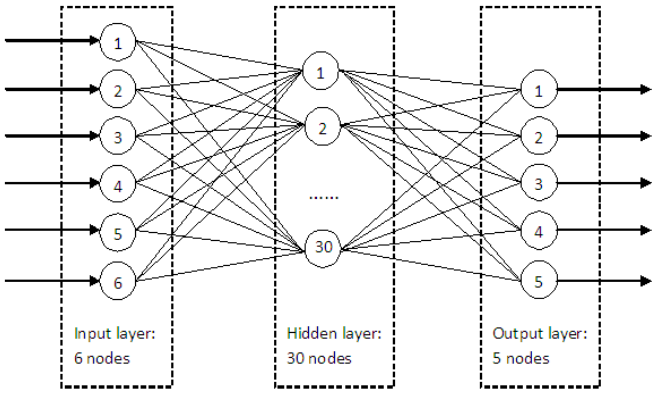

Figure 7: Driving Trend NN structure

TABLE IV
FIVE CLASSES OF DRIVING TRENDS

Driving Trend classes	description	Quantitative description
0	No speed	sp = 0
1	Low speed cruise	$0<sp_{ave}<58.65$ ft/s & $0.5<a_{ave}<0.5$ft/s^2
2	High speed cruise	$sp_{ave}>58.65$ ft/s & $0.5<a_{ave}<0.5$ft/s^2
3	Acceleration	$a_{ave}>0.5$ ft/s^2
4	Deceleration	$a_{ave}<0.5$ ft/s^2

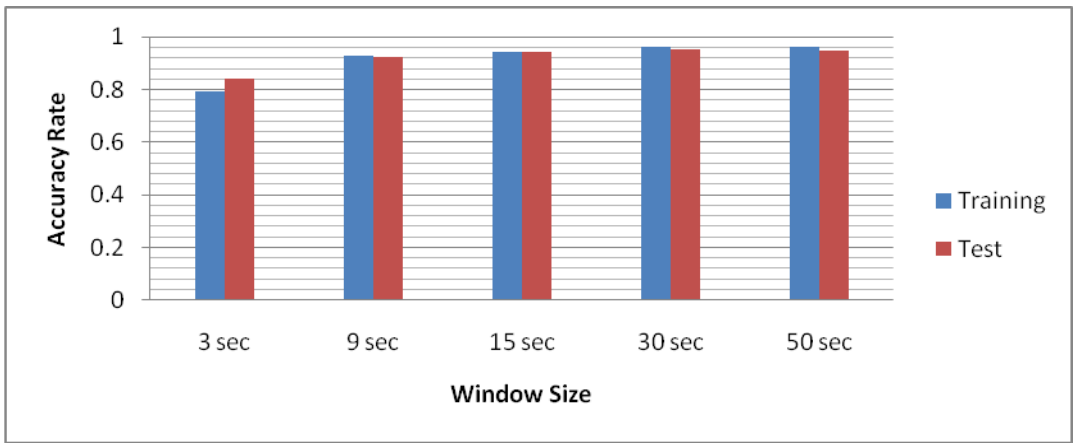

Figure 8. Performances of driving trend prediction neural network on various window sizes.

III.2 Machine learning of optimal energy management

A. Power split optimization using DP for each Facility Specific drive cycle

We applied the DP algorithm described in Section II to every Facility Specific (FS) drive cycle, R_i, i = 1,…,11, to find the optimal power settings associated with those roadway types and traffic congestion levels. The algorithm requires the use of a high fidelity vehicle system modeling and simulation program, such as PSAT or ADVISOR. Two major steps in the algorithm require the use of such a simulation program. First we used the simulation program to build a model of a particular vehicle of interest. Second, we run the vehicle model in the simulation program to generate step-by-step system state data: $P_{drive\text{-}sh}(t)$, $P_L(t)$ and $v_s(t)$, t=1, … , N, for every FC drive cycle.

A fuel rate matrix is generated for all possible combinations of the two control variables, battery power, P_{batt}, and engine speed, ω_{eng}, within the specific upper and lower bounds of P_{batt} and ω_{eng}, denoted as $P_{batt\_min}(t) \le P_{batt}(t) \le P_{batt\_max}(t)$ and $\omega_{eng\_min}(t) \le \omega_{eng}(t) \le \omega_{eng\_max}(t)$. The fuel rate matrix, $fuel\_rate(P_{batt}(t), \omega_{eng}(t) \mid P_{drive\_sh}(t), P_L(t))$, is generated for each time step t as a function of $P_{batt}(t)$ and $\omega_{eng}(t)$ for the given drivetrain power $P_{drive\text{-}sh}(t)$, and the electric load power $P_L(t)$. Then the DP optimization program described in Section II is applied to every one of the 11 standard FS drive cycles to obtain the optimal sequence of the two control variables, engine speed, ω_{eng} and battery power, P_{batt} pertaining to each drive cycle. Figure 9 summarizes the major computational steps in generating optimal operating points at every time step for every FS drive cycle.

Figure 10 shows the optimal P_{batt} and engine speed ω_{eng} generated by the DP for the Arterial LOS CD drive cycle and compared with the output generated by the default controller in the Ford Escape provided by PSAT. The detailed description of this vehicle model will be presented at the Part II of this paper series. Table V shows the performances of DP on all 11 Sierra drive cycles. For the purpose of comparison, we also listed the performance of the Ford Escape controller provided by the PSAT simulation model on these drive cycles as well. Since we cannot control the ending SOC for the Ford Escape controller in PSAT,

the ending SOC values vary from cycle to cycle. In order to make a fair comparison, we re-calculated the DP fuel cost with an SOC correction. Specifically, we reran the Dynamic Programming process by starting at 50% SOC and forcing the DP program to end at the same SOC of the Ford Escape controller in PSAT.

It is clear that the fuel savings from DP control is quite significant, ranging from 8.95% ~ 16.80%. However we need to point out that for in-vehicle implementation, DP cannot be used for real-time control since it requires the knowledge of the entire drive cycle. Furthermore, implementation of an optimal energy management in either Ford Escape or Toyota Prius needs to be traded-off with other vehicle attributes such as drivability, emission and OBD to make trade-offs. So DP result only serves as an upper bound of energy optimization in a vehicle for a given drive cycle.

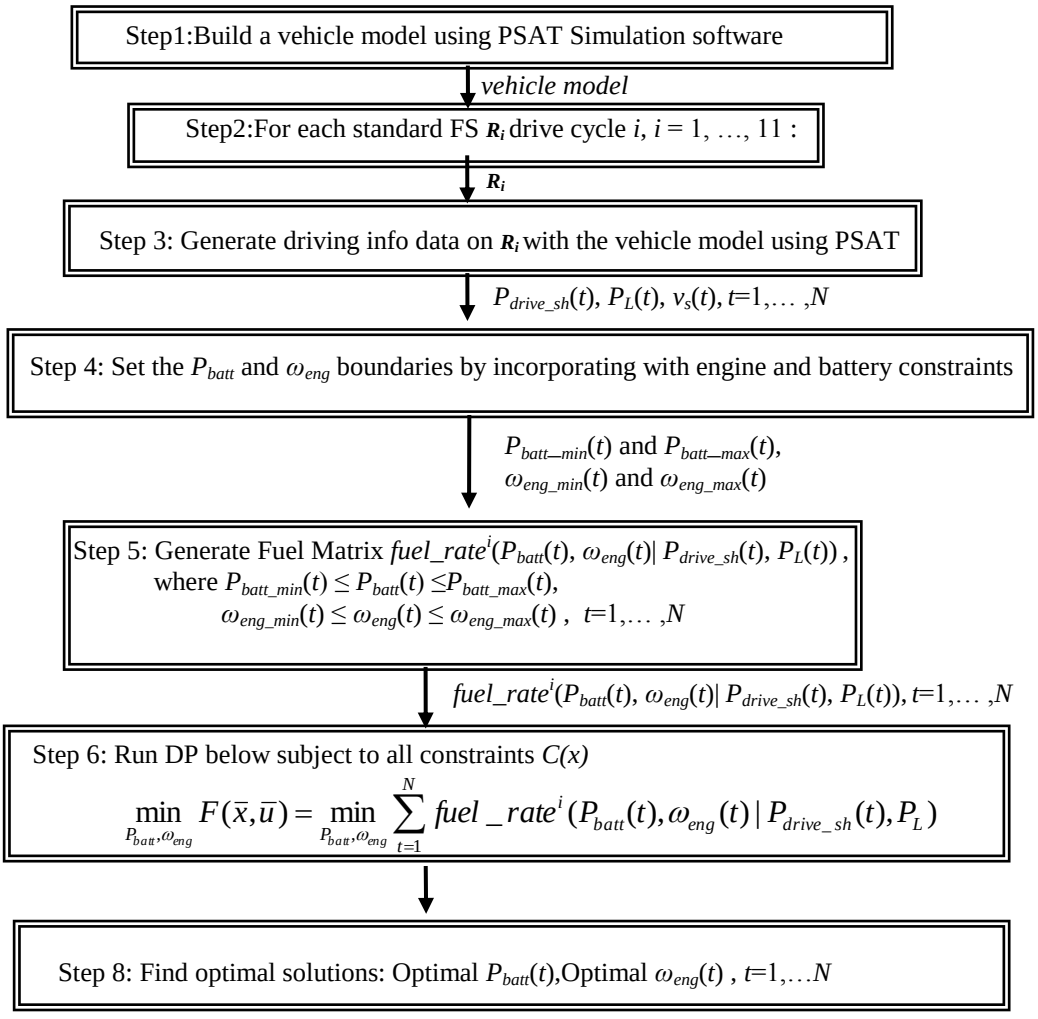

Figure. 9. Computational steps of DP optimization in a HEV.

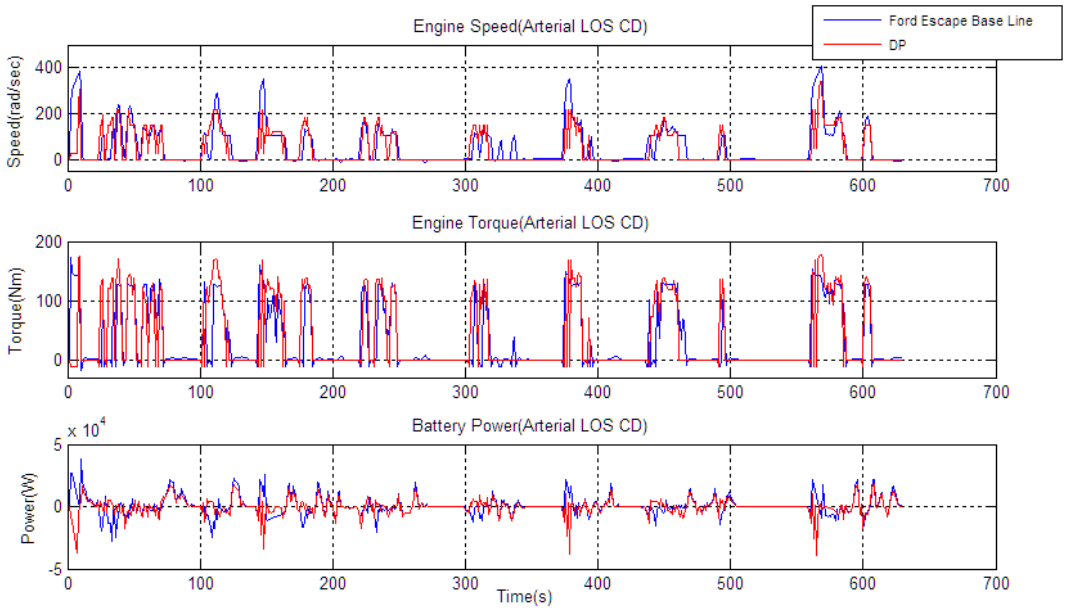

Figure 10. DP results with Ford Escape model in PSAT for Arterial LOS CD cycle.

TABLE V
PERFORMANCE OF DP OPTIMIZATION ON THE 11 SIERRA DRIVE CYCLES

Cycle	Cycle Time(s)	Fuel Consumption (g)		Saving by DP (%)
		DP	Ford Escape	
Freeway LOS A: R_1	400	747.99	895.64	16.48
Freeway LOS B: R_2	367	655.11	778.23	15.82
Freeway LOS C: R_3	449	795.40	947.02	16.01
Freeway LOS D: R_4	434	737.74	884.63	16.60
Freeway LOS E: R_5	472	619.80	744.98	16.80
Freeway LOS F: R_6	537	302.62	350.84	13.74
Freeway Ramps: R_7	270	198.16	237.98	16.73
Arterials LOS A-B: R_8	738	329.72	381.83	13.65
Arterials LOS C-D: R_9	630	229.45	262.57	12.61
Arterials LOS E-F: R_{10}	504	131.32	147.24	10.81
Local : R_{11}	526	133.63	146.75	8.95

B. Neural network training of optimal power solutions for Facility Specific drive cycles

Two sets of neural networks ($NN^i_{P_{bat}}$, $NN^i_{\omega_{eng}}$) have been developed to learn the optimal power split generated by the Dynamic Programming for each of the 11 roadway types and traffic congestion levels, R_i, i=1,…,11. The neural network, $NN^i_{P_{bat}}$ predicts P_{batt}, the optimal battery power, and the neural network, and $NN^i_{\omega_{eng}}$ predicts the optimal engine speed ω_{eng} for the roadway type and traffic congestion level R_i. The input variables to $NN^i_{P_{bat}}$ are $v_s(t)$, $P_{drive\text{-}sh}(t)$, $DT(t)$, and $SOC(t)$, where $v_s(t)$ is the vehicle speed, $P_{drive\_sh}(t)$ is the driver's power demand, $DT(t)$ is the driving trend, and $SOC(t)$ is the state of charge of the battery. $DT(t)$

can take one of the five states: no speed, low speed cruise, high speed cruise, acceleration and deceleration. The input variables to $NN^i_{\omega_{eng}}$ are $v_s(t)$, $P_{drive\text{-}sh}(t)$, and $SOC(t)$.

Figure 11 shows the architecture of the two neural networks, $NN^i_{P_{bat}}$ and $NN^i_{\omega_{eng}}$. For each standard FS drive cycle, R_i, i = 1, …, 11, the training data, Ω_i, for the two neural networks are generated by the procedure described in the last subsection. Here $\Omega_i = \{ v^i_s(t),\ P^i_{drive-sh}(t),\ DT^i(t), SOC^i(t),\ P^i_{batt}(t)\ ,\ \omega^i_{eng}(t) \mid t = 1, \ldots N^i\}$, where $v^i_s(t)$, $P^i_{drive-sh}(t)$, $DT^i(t), SOC^i(t)$ are the vehicle speed, driver power demand, driving trend and battery state of charge at time t respectively, and $P^i_{batt}(t)$, $\omega^i_{eng}(t)$ are the optimal battery power and engine speed settings generated by the DP algorithm at time t for drive cycle R_i. The variable N^i is the length of R_i. The neural networks as trained for different FS drive cycles can have different numbers of hidden nodes. The Performance of the NN training is measured by Mean Squared Errors (MSE) defined as:

$$MSE = \frac{1}{N}\sum_{t=1}^{N}(output(t) - tar(t))^2, \tag{19}$$

where *output(t)* is the NN output and *tar(t)* is the truth target value. Table VI shows the performance table in terms of MSE of the neural networks $NN^i_{P_{bat}}$ and $NN^i_{\omega_{eng}}$ as compared to the DP data for each of 11 Sierra FS cycles, R_i, i=1,..,11.

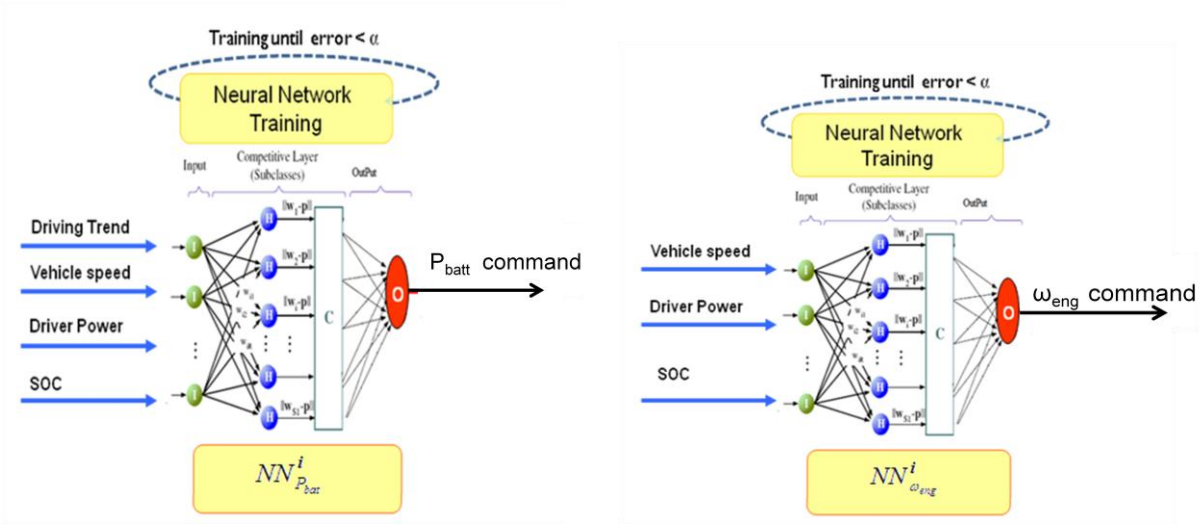

Figure 11. The energy management neural networks, $NN^i_{P_{bat}}$ and $NN^i_{\omega_{eng}}$ for Sierra FS cycle R_i, i=1,..,11.

Figure 12. Comparison of optimal engine speed and battery power generated by the neural networks and DP for Freeway LOS C.

TABLE VI.
PERFORMANCE OF NEURAL NETWORKS TRAINED FOR INTELLIGENT ENERGY MANAGEMENT

Cycle	NN_{Pbatt} (MSE)	NN_{weng} (MSE)		Cycle	NN_{Pbatt} (MSE)	NN_{weng} (MSE)
Freeway LOS A	0.0012	0.0009		Ramp	0.0004	0.0009
Freeway LOS B	0.0015	0.0012		Local	0.0004	0.0002
Freeway LOS C	0.0012	0.0006		Arterial LOS AB	0.0007	0.0007
Freeway LOS D	0.0008	0.0006		Arterial LOS CD	0.0005	0.0003
Freeway LOS E	0.0011	0.0007		Arterial LOS EF	0.0007	0.0006
Freeway LOS F	0.0007	0.0005		All 11 cycles	0.0013	0.0008

Figure 12 shows the battery power, P_{batt}, (top graph) and engine speed, ω_{eng}, (bottom graph) generated by the trained neural networks and DP on a R_3 drive cycle, i.e. Freeway LOS C. It can be observed that the results generated by the neural networks are very close to the results generated by DP, which is an optimal algorithm, but cannot be implemented for real-time operation.

In the Part II of this paper series, we will present an intelligent energy controller that uses, in real-time, the NN_RT&TC to predict the current roadway type and traffic congestion level, NN_DT to predict the driving trend, and then, assume the predicted roadway type is R_i, use the two energy control neural networks, $NN^i_{P_{bat}}$ and $NN^i_{\omega_{eng}}$ trained for the roadway type R_i to generate the optimal battery power and engine speed, throughout the drive cycle.

IV. CONCLUSION

We presented a machine learning framework, ML_EMO_HEV, for the optimization of energy management in an HEV. This framework includes machine learning algorithms for predicting roadway types and traffic congestion levels and driving trends and then using these predicted values in another algorithm that learns optimal energy settings based on the predicted roadway types and traffic congestion levels and driving trends. The neural network, NN_RT&TC, was designed and trained for the prediction of roadway types and traffic congestion levels. It is a multi-class neural network trained to predict which of the 11 standard FS drive cycles the current roadway type and traffic congestion level belongs to. Its performance on 10 test drive cycles has accuracy within the range of 91.6% and 98.7%. The neural network that predicts the driving trend, NN_DT, predicts one of five classes of driving trend: no speed, low speed cruise, high speed cruise, acceleration and deceleration. Its performance for a 9 second window is approximately 94% in accuracy for both training and test data. For each of the 11 Sierra FS drive cycles, two neural networks were trained, one to emulate the optimal engine speed generated by DP and the other the optimal battery power. The performance of the neural networks for generating the optimal engine speed over all 11 roadway types and traffic congestion levels have an MSE ranging between 0.0002 and 0.0012. The neural networks for generating the optimal battery power have an MSE ranging between 0.0004 and 0.0015. In the second paper in the series, we will present an intelligent online power controller developed under ML_EMO_HEV, and its performances in a target vehicle under various training conditions and drive cycles.

ACKNOWLEDGMENT

This work was supported in part by a grant from the State of Michigan under the 21st Jobs Fund and a grant from the Institute of Advanced Vehicle Systems at the University of Michigan-Dearborn.

REFERENCES

[1] K Wipke, T Markel, and D Nelson, "Optimizing Energy Management Strategy and Degree of Hybridization for a Hydrogen Fuel Cell SUV," *Proceedings of 18th Internation Electric Vehicle Symposium (EVS 18)*, Berlin, 2001.

[2] S. Jeon, S. Jo, Y. Park, J. Lee, "Multi-Mode Driving Control of a Parallel Hybrid Electric Vehicle Using Driving Pattern Recognition," *ASME Journal of Dynamic Systems, Measurement, and Control*, Vol. 124, No. 1, pp. 141-149, 2002.

[3] Y. Zhu, Y Chen, Z. Wu, A. Wang, "Optimization design of an energy management strategy for hybrid vehicles," International Journal of Alternative Propulsion 2006 - Vol. 1, No.1 pp. 47 - 62.

[4] Y. Zhu, Y. Chen, and Q. Chen, "Analysis and Design of an Optimal Energy Management and Control System for Hybrid Electric Vehicles," Proc. of the 19th Electric Vehicles Symposium, Busan, Korea, 2002.

[5] N. Schouten, M. Salman, N. Kheir, "Fuzzy Logic Control for Parallel Hybrid Vehicles," *IEEE Transactions on Control Systems Technology*, Vol. 10, No. 3, pp460-468, 2002.

[6] E. D. Tate and S. P. Boyd, "Finding ultimate limits of performance for hybrid electric vehicles," *Society of Automotive Engineers Paper*-01-3099, 2000.

[7] S. Delprat, J. Lauber, T.M. Guerra, and J. Rimaux, "Control of a parallel hybrid powertrain: optimal control," *IEEE Transactions on Vehicular Technology* , vol. 53, no. 3, pp. 872–881, May 2004.

[8] C.-C. Lin, H. Peng, J.W. Grizzle, and J.-M. Kang, "Power management strategy for a parallel hybrid electric truck," *IEEE Transactions on Control System Technology*, vol. 11, no. 6, pp. 839–849, Nov. 2003.

[9] T. Hofman and R. van Druten, "Energy analysis of hybrid vehicle powertrains," in *Proc. IEEE Int. Symp. Veh. Power Propulsion*, Paris, France, Oct. 2004.

[10] I. Arsie, M. Graziosi, C. Pianese, G. Rizzo, and M. Sorrentino, "Optimization of supervisory control strategy for parallel hybrid vehicle with provisional load estimate," in *Proc. 7th Int. Symp. Adv. Vehicle Control (AVEC)*, Arnhem, the Netherlands, Aug. 2004.

[11] G. Paganelli, G. Ercole, A. Brahma, Y. Guezennec, and G. Rizzoni, "General supervisory control policy for the energy optimization of charge-sustaining hybrid electric vehicles," *Society of Automotive Engineers of Japan Rev.*, vol. 22, no. 4, pp. 511–518, Apr. 2001.

[12] V. H. Johnson, K. B.Wipke, and D. J. Rausen, "HEV control strategy for real-time optimization of fuel economy and emissions," *Society of Automotive Engineers Paper*-01-1543, 2000.

[13] A. Sciarretta, L. Guzzella, and M. Back, "A real-time optimal control strategy for parallel hybrid vehicles with on-board estimation of the control parameters," in *Proc. IFAC Symp. Adv. Automotive Contr.*, Salerno, Italy, Apr. 19–23, 2004.

[14] C. Lin, H. Peng, J. Grizzle, "A Stochastic Control Strategy for Hybrid Electric Vehicles," *Proceeding of the American Control conference*, Boston, Massachusetts,2004.

[15] E. Ericsson, "Variability in urban driving patterns," *Transportation Res. Part D*, vol. 5, pp. 337–354, 2000.

[16] E. Ericsson, "Independent driving pattern factors and their influence on fuel-use and exhaust emission factors," *Transportation Res. Part D*, vol. 6, pp. 325–341, 2001.

[17] S.-I. Jeon, S. -T. Jo, Y. -I. Park, and J. -M. Lee, "Multi-mode driving control of a parallel hybrid electric vehicle using driving pattern recognition," *J. Dyn. Syst., Measure. Contr.*, vol. 124, pp. 141–149, Mar. 2002.

[18] Langari, R.; Jong-Seob Won, **"**Intelligent energy management agent for a parallel hybrid vehicle-part I: system architecture and design of the driving situation identification process," *IEEE Transactions on Vehicular Technology*, vol. 54, issue 3, pp. 925 – 934, 2005.

[19] Jong-Seob Won; Langari, R., "Intelligent energy management agent for a parallel hybrid vehicle-part II: torque distribution, charge sustenance strategies, and performance results," *IEEE Transactions on Vehicular Technology*, vol. 54, issue 3, pp. 935 – 953, 2005.

[20] F.U. Syed et al., "Derivation and Experimental Validation of a Power-Split Hybrid Electric Vehicle Model," *IEEE Transactions on Vehicular Technology*, vol. 55, 2006, p. 1731.

[21] M. Kuang, D. Hrovat, "Hybrid Electric Vehicle Powertrain Modeling and Validation", Proc. of EVS 14, the 20th International Electric Vehicle Symposium and Exposition, Nov., 2003.

[22] M. Koot, "Energy Management for vehicular electric power systems,"Thesis, Technische Universiteit Eindhoven, 2006.

[23] T. R. Carlson and R. C. Austin, "Development of speed correction cycles," Sierra Research, Inc., Sacramento, CA, Report SR97-04-01, 1997.

[24] Sierra Research," SCF Improvement – Cycle Development," Sierra Report No. SR2003-06-02, 2003.

[25] Highway Capacity Manual 2000, Transportation Res. Board, Wash., DC, 2000.

[26] Jungme Park, ZhiHang Chen, Leonidas Kiliaris, Ming Kuang, Abul Masrur, Anthony Phillips and Yi L. Murphey," Intelligent vehicle power control based on machine learning of optimal control parameters and prediction of road type and traffic congestions," IEEE Transactions on Vehicular Technology, Vol 58, No. 9, November, 2009.